Inorg. Chem. **2008**, *47*, 7430−7437

$ZnVSe_2O_7$ and $Cd_6V_2Se_5O_{21}$: New d^{10} Transition-Metal Selenites with V(IV) or V(V) Cations

Hai-Long Jiang,[†,‡] Fang Kong,[†,‡] Yang Fan,[†,‡] and Jiang-Gao Mao*[,†]

State Key Laboratory of Structural Chemistry, Fujian Institute of Research on the Structure of Matter, Chinese Academy of Sciences, Fuzhou 350002, P. R. China, and Graduate School of the Chinese Academy of Sciences, Beijing, 100039, P. R. China

Received April 8, 2008

Two new metal selenites with a combination of vanadium(IV) or vanadium(V) cations, namely, $ZnVSe_2O_7$ and $Cd_6V_2Se_5O_{21}$, have been synthesized by hydrothermal and high-temperature solid-state reactions, respectively. The structure of $ZnVSe_2O_7$ features a 3D network of vanadium(IV) selenite with 1D tunnels occupied by zinc(II) ions. The 3D network of vanadium(IV) selenite is formed by corner-sharing $V^{IV}O_6$ octahedral chains bridged by selenite groups. In $Cd_6V_2Se_5O_{21}$, the interconnection of cadmium(II) ions by bridging and chelating selenite groups led to a 3D framework with large tunnels along the *b* axis, and the 1D chains of corner-sharing $V^{V}O_4$ tetrahedra are inserted in the above large tunnels and are bonded to the cadmium selenite framework via Cd−O−V bridges. Both compounds exhibit broad emission bands in the blue-light region. Results of magnetic property measurements show there is significant antiferromagnetic interaction between V^{4+} centers in $ZnVSe_2O_7$. The electronic structure calculations for both compounds have been also performed.

Introduction

Cations with stereochemically active lone-pair electrons such as Se^{4+} and Te^{4+} are of great research interest owing to their asymmetric coordination environments caused by so-called second-order Jahn−Teller (SOJT) distortion, which may give rise to non-centrosymmetric structures (NCS) with possible second-harmonic generation (SHG).[1] The combination of lone-pair cations with transition-metal ions with d^0 electronic configurations such as Mo^{6+} and W^{6+}, which are also susceptible to SOJT distortion, is reported to form a number of compounds with excellent SHG properties due to the additive polarization of both types of bonds.[1−10] Because of the higher coordination numbers for the lanthanide ions, the corresponding lanthanide compounds containing both types of SOJT distortion effects are rarely

* To whom correspondence should be addressed. E-mail: mjg@fjirsm.ac.cn.

† Fujian Institute of Research on the Structure of Matter, Chinese Academy of Sciences.

‡ Graduate School of the Chinese Academy of Sciences.

(1) (a) Wickleder, M. S. *Chem. Rev.* **2002**, *102*, 2011. (and references therein). (b) Ok, K. M.; Halasyamani, P. S. *Chem. Soc. Rev.* **2006**, *35*, 710.

(2) (a) Ok, K. M.; Halasyamani, P. S. *Chem. Mater.* **2006**, *18*, 3176. (b) Halasyamani, P. S. *Chem. Mater.* **2004**, *16*, 3586. (c) Kong, F.; Huang, S.-P.; Sun, Z.-M.; Mao, J.-G.; Cheng, W.-D. *J. Am. Chem. Soc.* **2006**, *128*, 7750.

(3) (a) Porter, Y.; Bhuvanesh, N. S. P.; Halasyamani, P. S. *Inorg. Chem.* **2001**, *40*, 1172. (b) Porter, Y.; Ok, K. M.; Bhuvanesh, N. S. P.; Halasyamani, P. S. *Chem. Mater.* **2001**, *13*, 1910. (c) Ok, K. M.; Bhuvanesh, N. S. P.; Halasyamani, P. S. *Inorg. Chem.* **2001**, *40*, 1978.

(4) (a) Porter, Y.; Halasyamani, P. S. *J. Solid State Chem.* **2003**, *174*, 441. (b) Harrison, W. T. A.; Dussack, L. L.; Jacobson, A. J. *Inorg. Chem.* **1994**, *33*, 6043. (c) Chi, E. O.; Ok, K. M.; Porter, Y.; Halasyamani, P. S. *Chem. Mater.* **2006**, *18*, 2070. (d) Balraj, V.; Vidyasagar, K. *Inorg. Chem.* **1998**, *37*, 4764.

(5) (a) Kim, J.-H.; Baek, J.; Halasyamani, P. S. *Chem. Mater.* **2007**, *19*, 5637. (b) Goodey, J.; Broussard, J.; Halasyamani, P. S. *Chem. Mater.* **2002**, *14*, 3174. (c) Goodey, J.; Ok, K. M.; Broussard, J.; Hofmann, C.; Escobedo, F. V.; Halasyamani, P. S. *J. Solid State Chem.* **2003**, *175*, 3. (d) Harrison, W. T. A.; Dussack, L. L.; Jacobson, A. J. *J. Solid. State Chem.* **1996**, *125*, 234. (e) Ra, H. S.; Ok, K. M.; Halasyamani, P. S. *J. Am. Chem. Soc.* **2003**, *125*, 7764.

(6) (a) Vaughey, J.-T.; Harrison, W. T. A.; Dussack, L. L.; Jacobson, A. J. *Inorg. Chem.* **1994**, *33*, 4370. (b) Kwon, Y.-U.; Lee, K.-S.; Kim, Y.-H. *Inorg. Chem.* **1996**, *35*, 1161. (c) Lee, K.-S.; Kwon, Y.-U.; Namgung, H.; Kim, S.-W. *Inorg. Chem.* **1995**, *34*, 4178.

(7) (a) Sivakumar, T.; Ok, K. M.; Halasyamani, P. S. *Inorg. Chem.* **2006**, *45*, 3602. (b) Ok, K. M.; Halasyamani, P. S. *Inorg. Chem.* **2005**, *44*, 3919. (c) Muller-Buschbaum, H.; Wedel, B. *Z. Naturforsch.* **1996**, *B51*, 1411. (d) Ok, K. M.; Zhang, L.; Halasyamani, P. S. *J. Solid State Chem.* **2003**, *175*, 264.

(8) (a) Shen, Y. L.; Jiang, H. L.; Xu, J.; Mao, J. G.; Cheah, K. W. *Inorg. Chem.* **2005**, *44*, 9314. (b) Jiang, H. L.; Ma, E.; Mao, J. G. *Inorg. Chem.* **2007**, *46*, 7012.

(9) Jiang, H. L.; Xie, Z.; Mao, J. G. *Inorg. Chem.* **2007**, *46*, 6495.

(10) (a) Kim, Y.-T.; Kim, Y.-H.; Park, K.; Kwon, Y.-U.; Young, V. G., Jr. *J. Solid. State Chem.* **2001**, *161*, 23. (b) Jiang, H.-L.; Huang, S.-P.; Fan, Y.; Mao, J.-G.; Cheng, W.-D. *Chem.—Eur. J.* **2008**, *14*, 1972. (c) Halasyamani, P. S.; O'Hare, D. *Inorg. Chem.* **1997**, *36*, 6409.

10.1021/ic800638e CCC: $40.75 © 2008 American Chemical Society
Published on Web 06/24/2008

SHG active, but exhibit strong luminescence in visible or the near-IR region.[8] So far, such studies are dominated by the alkali (alkaline earth, lanthanide)-Se(IV)(or Te(IV))-Mo^{6+}/W^{6+} combinations,[3–6,8] and a few compounds containing pentavalent cations (V^{5+} or Nb^{5+} and Ta^{5+}).[7,10] So far, only a few compounds of the transition metal (TM)-d^0 TM-Se(IV)(or Te(IV))-oxide systems were reported.[9,10] $Ni_3(Mo_2O_8)(XO_3)$ (X = Se, Te) were found to display two different types of 3D structures containing $[Mo_4O_{16}]^{8-}$ clusters and $[Ni_6O_{22}]^{32-}$ clusters or 1D nickel oxide chains.[9] $Cd(VO_2)_4(SeO_3)_3 \cdot H_2O$ with a pillar-layered structure was reported,[10a] the layer is composed of dimers of VO_5 square pyramids and dimers of CdO_7 polyhedra connected to one another by corner and/or edge sharing, whereas the pillars are composed of distorted VO_6 octahedra connected to one another via corner and edge sharing with capping selenite groups. Very recently, $Zn_3V_2TeO_{10}$ and $Cd_4V_2Te_3O_{15}$ were also reported by our group.[10b] The structure of $Zn_3V_2TeO_{10}$ is a complicated 3D network constructed by ZnO_5, ZnO_6, VO_4, and TeO_4 polyhedra interconnected via corner- and edge- sharing whereas $Cd_4V_2Te_3O_{15}$ with an SHG response of about 1.4 times of KDP features a 3D network composed of layers of cadmium tellurite further bridged by both isolated VO_4 tetrahedra and 1D vanadium−oxide helical chains. It is interesting to note that the V^{5+} cation can display three types of coordination geometries (tetrahedron, square pyramid, and octahedron),[10] whereas the Mo^{6+} and W^{6+} cations are normally octahedrally or tetrahedrally coordinated. Therefore, it is anticipated that a variety of new compounds with interesting structures and properties can be discovered in the transition-metal V^{5+}-selenite and -tellurite systems. As an extension of our previous studies on new compounds in the d^{10} TM−V−Se(Te)−O systems, two new quaternary phases, namely, $ZnVSe_2O_7$ and $Cd_6V_2Se_5O_{21}$, have been successfully obtained. Herein, we report their syntheses, crystal and band structures, as well as properties.

Experimental Section

Materials and Instrumentation. All of the chemicals were of analytically pure from commercial sources and used without further purification. Transition-metal oxides were purchased from the Shanghai Reagent Factory, and SeO_2 (99+%) was purchased from ACROS ORGANICS. Chemical composition analyses were performed on a field emission scanning electron microscope (FESEM, JSM6700F) equipped with an energy dispersive X-ray spectroscope (EDS, Oxford INCA). The UV absorption spectra were recorded on a PE Lambda 900 UV−vis spectrophotometer in the wavelength range of 200−1800 nm. The absorption spectra were determined by the diffuse-reflectance technique.[11] $F(R)$ and R are linked by $F(R) = (1 - R)^2/2R$, where R is the reflectance and $F(R)$ is the Kubelka−Munk remission function. The minima in the second-derivative curves of the Kubelka−Munk function are taken as the position of the absorption bands. X-ray powder diffraction (XRD) patterns were collected on a XPERT-MPD θ-2θ diffractometer. IR spectra were recorded on a Magna 750 FTIR spectrometer as KBr pellets in the range of 4000−400 cm^{-1}. Thermogravimetric analyses (TGA) were carried out with a NETZSCH STA 449C unit, at a heating rate of 10 °C/min under a static air atmosphere. Photoluminescence analysis was performed on a PerkinElmer LS55 fluorescence spectrometer. EPR spectra were collected on powder samples at the X-band frequency with a Bruker ER-420 spectrometer at room temperature. Magnetic susceptibility measurements on polycrystalline samples were performed with a PPMS-9T magnetometer at a field of 5000 Oe in the range of 2 to 300 K. The raw data were corrected for the susceptibility of the container and the diamagnetic contributions of the sample using Pascal constants.

Table 1. Summary of Crystal Data and Structural Refinements for $ZnVSe_2O_7$ and $Cd_6V_2Se_5O_{21}$

formula	$ZnVSe_2O_7$	$Cd_6V_2Se_5O_{21}$
fw	386.23	1507.08
cryst syst	monoclinic	monoclinic
space group	$P2_1/n$	$P2_1/c$
a/Å	7.442(3)	15.301(6)
b/Å	12.530(4)	5.437(2)
c/Å	7.480(3)	23.816(10)
α/deg	90	90
β/deg	117.066(4)	93.950(4)
γ/deg	90	90
V/Å^3	621.1(4)	1976.6(13)
Z	4	4
D_{calcd}/g·cm^{-3}	4.131	5.064
μ(Mo Kα)/mm^{-1}	17.072	16.536
GOF on F^2	0.998	1.110
R1, wR2 [$I > 2\sigma(I)$][a]	0.0216, 0.0481	0.0476, 0.0825
R1, wR2 (all data)	0.0258, 0.0488	0.0682, 0.0900

[a] $R1 = \sum||F_o| - |F_c||/\sum|F_o|$, $wR2 = \{\sum w[(F_o)^2 - (F_c)^2]^2/\sum w[(F_o)^2]^2\}^{1/2}$.

Preparation of $ZnVSe_2O_7$. A mixture of $Zn(CH_3COO)_2 \cdot 2H_2O$ (0.134 g, 0.84 mmol), V_2O_5 (0.051 g, 0.28 mmol), SeO_2 (0.186 g, 1.08 mmol), and H_2O (5 mL) was sealed in an autoclave equipped with a Teflon liner (23 mL) and heated at 200 °C for 4 days, followed by slow cooling to room temperature at a rate of 6 °C/hr. Dark-cyan prism-shaped crystals of $ZnVSe_2O_7$ in ca. 33% yield (based on Zn), and a few green plate-shaped crystals of $V_2Se_2O_8 \cdot 2H_2O$ were recovered. It is found that V^{5+} ion was reduced to V^{4+} ion, probably by the reducing SeO_2. To prepare its monophase product and improve the yield, VO_2 was used directly as the starting material. A mixture of $Zn(CH_3COO)_2 \cdot 2H_2O$ (0.162 g, 0.74 mmol), VO_2 (0.031 g, 0.37 mmol), and SeO_2 (0.206 g, 1.85 mmol) in 5 mL H_2O was allowed to react under the same conditions previously described, and crystals of $ZnVSe_2O_7$ were obtained in ca. 45% yield (based on zinc,Supporting Information). Results of microprobe elemental analyses on several single crystals gave a molar ratio of Zn/V/Se of 1.1:1.0:2.2, which is in good agreement with the one determined from single-crystal X-ray structural analysis.

Preparation of $Cd_6V_2Se_5O_{21}$. Red needle-shaped single crystals of $Cd_6V_2Se_5O_{21}$ could be obtained by the solid-state reaction of a mixture composed of CdO, V_2O_5, and SeO_2 in a molar ratio of 2:1:1 or 1:1:1. The reaction mixture was thoroughly ground and pressed into a pellet, sealed into an evacuated quartz tube. The tube was heated at 300 °C for one day and at 680 °C for 6 days, then slowly cooled to 280 at 4 °C/h and finally cooled to room temperature in 10 h. Results of the EDS microprobe elemental analyses on several single crystals gave a molar ratio of Cd/V/Se of 6.2:2.0:5.3, which is close to the one determined from single-crystal X-ray diffraction studies. After structural analysis, the single-phase product of $Cd_6V_2Se_5O_{21}$ was obtained quantitatively by reacting a mixture of $CdO/V_2O_5/SeO_2$ in a molar ratio of 6:1:5 at 650 °C for 6 days (Supporting Information).

(11) Kubelka, P.; Munk, F. *Z. Tech. Phys.* **1931**, *12*, 593.
(12) (a) *CrystalClear ver. 1.3.5.*, Rigaku Corp.: Woodlands, TX, 1999. (b) Sheldrick, G. M. *SHELXTL, Crystallographic Software Package, SHELXTL, Version 5.1*; Bruker-AXS: Madison, WI, 1998.

Table 2. Important Bond Lengths (Angstroms) for $ZnVSe_2O_7$ and $Cd_6V_2Se_5O_{21}$[a]

	$ZnVSe_2O_7$		
Zn(1)−O(3)#1	1.957(3)	Zn(1)−O(6)	2.011(2)
Zn(1)−O(6)#2	2.057(2)	Zn(1)−O(1)	2.076(2)
Zn(1)−O(2)	2.150(2)	V(1)−O(7)	1.611(3)
V(1)−O(5)#3	1.964(2)	V(1)−O(4)	1.969(2)
V(1)−O(2)	2.005(2)	V(1)−O(1)#4	2.005(2)
V(1)−O(7)#5	2.318(3)	Se(1)−O(3)	1.658(3)
Se(1)−O(2)	1.718(2)	Se(1)−O(1)	1.743(2)
Se(2)−O(5)	1.681(2)	Se(2)−O(4)	1.690(3)
Se(2)−O(6)	1.723(2)		
	$Cd_6V_2Se_5O_{21}$		
Cd(1)−O(21)#1	2.237(6)	Cd(1)−O(7)	2.239(6)
Cd(1)−O(4)#2	2.250(6)	Cd(1)−O(18)	2.341(7)
Cd(1)−O(20)#3	2.515(6)	Cd(1)−O(8)#3	2.526(6)
Cd(2)−O(6)	2.194(7)	Cd(2)−O(10)	2.253(6)
Cd(2)−O(2)	2.286(6)	Cd(2)−O(1)	2.306(6)
Cd(2)−O(13)	2.312(6)	Cd(2)−O(12)	2.671(6)
Cd(3)−O(3)#4	2.191(7)	Cd(3)−O(10)	2.222(6)
Cd(3)−O(17)	2.335(6)	Cd(3)−O(2)#4	2.394(6)
Cd(3)−O(3)	2.477(7)	Cd(3)−O(2)#3	2.492(6)
Cd(3)−O(12)#3	2.519(6)	Cd(4)−O(8)#5	2.299(6)
Cd(4)−O(4)	2.326(6)	Cd(4)−O(9)#6	2.328(6)
Cd(4)−O(7)#7	2.426(6)	Cd(4)−O(15)	2.486(7)
Cd(4)−O(7)#6	2.498(6)	Cd(4)−O(5)	2.535(6)
Cd(4)−O(8)#7	2.615(6)	Cd(5)−O(1)	2.199(6)
Cd(5)−O(15)#3	2.263(6)	Cd(5)−O(9)#6	2.266(6)
Cd(5)−O(5)	2.315(6)	Cd(5)−O(4)#3	2.263(6)
Cd(5)−O(13)	2.618(6)	Cd(6)−O(12)#3	2.284(6)
Cd(6)−O(11)#6	2.314(6)	Cd(6)−O(14)#3	2.317(6)
Cd(6)−O(11)	2.355(6)	Cd(6)−O(13)	2.383(6)
Cd(6)−O(14)#6	2.421(6)	V(1)−O(16)	1.781(6)
V(1)−O(17)	1.650(7)	V(1)−O(18)	1.642(6)
V(1)−O(19)	1.776(7)	V(2)−O(16)#8	1.795(6)
V(2)−O(19)	1.767(7)	V(2)−O(20)	1.638(6)
V(2)−O(21)	1.668(7)	Se(1)−O(3)	1.695(7)
Se(1)−O(1)	1.701(6)	Se(1)−O(2)#3	1.716(6)
Se(2)−O(5)	1.685(6)	Se(2)−O(6)	1.684(6)
Se(2)−O(4)	1.754(6)	Se(3)−O(9)	1.687(6)
Se(3)−O(8)	1.701(6)	Se(3)−O(7)	1.724(6)
Se(4)−O(11)	1.677(6)	Se(4)−O(10)	1.708(6)
Se(4)−O(12)	1.720(6)	Se(5)−O(15)	1.682(6)
Se(5)−O(14)	1.687(6)	Se(5)−O(13)	1.739(6)

[a] For $ZnVSe_2O_7$: #1 $-x, -y+1, -z$; #2 $-x+1, -y+1, -z$; #3 $x-1/2, -y+1/2, z+1/2$; #4 $-x+1/2, y-1/2, -z+1/2$; #5 $x-1/2, -y+1/2, z-1/2$. For $Cd_{>6}V_2Se_5O_{21}$: #1 $-x+2, y+1/2, -z+3/2$; #2 $x+1, y+1, z$; #3 $x, y+1, z$; #4 $-x+1, y+1/2, -z+3/2$; #5 $-x+1, -y, -z+1$; #6 $-x+1, -y+1, -z+1$; #7 $x-1, y, z$; #8 $x, y-1, z$.

Single-Crystal Structure Determination. Data collections for both compounds were performed on a Rigaku Mercury CCD diffractometer equipped with a graphite-monochromated Mo−Kα radiation ($\lambda = 0.71073$ Å) at 293 K. Both data sets were corrected for Lorentz and polarization factors as well as for absorption by Multiscan method.[12a] Both structures were solved by the direct methods and refined by full-matrix least-squares fitting on F^2 by *SHELX-97*.[12b] All of the atoms were refined with anisotropic thermal parameters. Crystallographic data and structural refinements for both compounds are summarized in Table 1. Important bond distances are listed in Table 2. More details on the crystallographic studies as well as atomic displacement parameters are given as Supporting Information.

Computational Descriptions. The crystallographic data of both compounds were used for the band structure calculations. The ab initio band structure calculations were performed with the total-energy code *CASTEP*.[13] The total energy is calculated with density functional theory (DFT) using Perdew−Burke−Ernzerhof generalized gradient approximation.[14a] The interactions between the ionic cores and the electrons are described by the norm-conserving pseudopotential.[14b] The following orbital electrons are treated as valence electrons: Cd-$4d^{10}5s^2$, Zn-$3d^{10}4s^2$, V-$3d^34s^2$, Se-$4s^24p^4$, and O-$2s^22p^4$. Considering the balance of computational cost and precision, we choose a cutoff energy of 460 and 450 eV for $ZnVSe_2O_7$ and $Cd_6V_2Se_5O_{21}$, respectively. Spin polarization was included for the electronic structure calculations of $ZnVSe_2O_7$. The other calculating parameters used in the calculations and convergent criteria were set by the default values of the *CASTEP* code.[13]

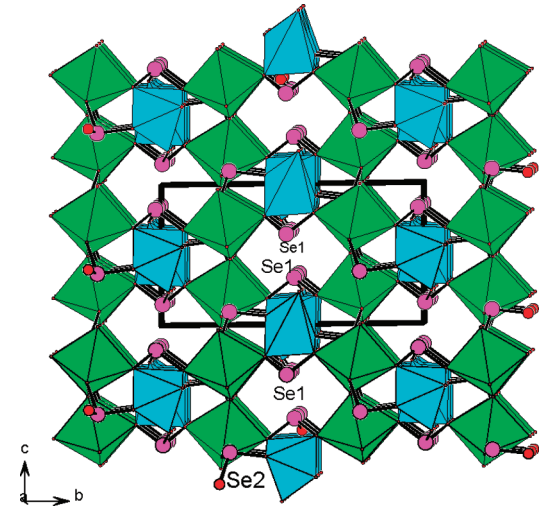

Figure 1. View of the structure of $ZnVSe_2O_7$ down the *a* axis. ZnO_5 trigonal bipyramids and VO_6 octahedra are shaded in cyan and green, respectively. Selenium and oxygen atoms are drawn as pink and red circles, respectively.

Results and Discussion

Two new zinc(II) or cadmium(II) vanadium selenites, namely, $ZnVSe_2O_7$ and $Cd_6V_2Se_5O_{21}$, have been successfully prepared by hydrothermal synthetic technique or high-temperature solid-state reaction. Both compounds exhibit new types of 3D architectures. Under hydrothermal condition, the V^{5+} ion could be reduced to V^{4+} as in our initial synthesis of $ZnVSe_2O_7$. This is probably due to the oxidation of some Se(IV) cations to Se(VI). Such phenomenon has been reported during the preparation of $VO(SeO_3)\cdot H_2O$ by hydrothermal reaction of V_2O_5 and H_2SeO_3.[15]

The structure of $ZnVSe_2O_7$ features a 3D network composed of 3D anionic $\{VSe_2O_7\}^{2-}$ with the zinc(II) cation occupying the 6MR tunnels along *a* axis (Figure 1). There are one zinc(II), one VO^{2+}, and two selenite anions in the asymmetric unit of $ZnVSe_2O_7$; hence, $ZnVSe_2O_7$ can also be formulated as $Zn(VO)(SeO_3)_2$. The zinc(II) ion is in a trigonal bipyramid geometry composed of five oxygens from four selenite groups with Zn−O distances ranging from 1.958(3) to 2.150(3) Å. The vanadium(IV) atom is octahedrally coordinated by six oxygen atoms from four selenite

(13) (a) Segall, M. D.; Lindan, P. L. D.; Probert, M. J.; Pickard, C. J.; Hasnip, P. J.; Clark, S. J.; Payne, M. C. *J. Phys.: Condens. Matter* **2002**, *14*, 2717. (b) Segall, M.; Lindan, P.; Probert, M.; Pickard, C.; Hasnip, P.; Clark, S.; Payne, M. *Materials Studio CASTEP, version 2.2*, 2002. (c) Milman, V.; Winkler, B.; White, J. A.; Pickard, C. J.; Payne, M. C.; Akhmatskaya, E. V.; Nobes, R. H. *Int. J. Quantum Chem.* **2000**, *77*, 895.

(14) (a) Perdew, J. P.; Burke, K.; Ernzerhof, M. *Phys. Rev. Lett.* **1996**, *77*, 3865. (b) Lin, J. S.; Qteish, A.; Payne, M. C.; Heine, V. *Phys. Rev.* **1993**, *B 47*, 4174.

(15) Huan, G.-H.; Johnson, J. W.; Jacobson, A. J.; Goshorn, D. P. *Chem. Mater.* **1991**, *3*, 539.

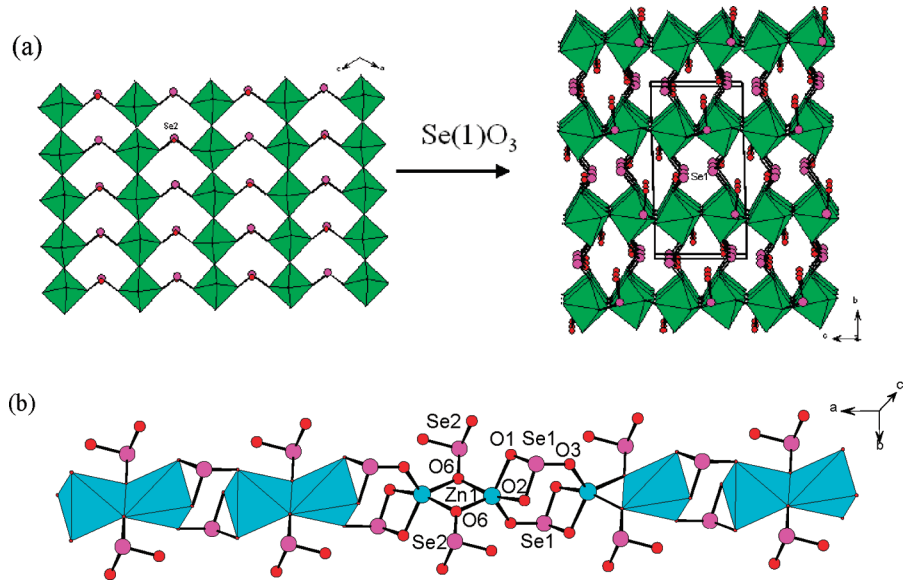

Figure 2. The V(1)−O−Se(2) layer parallel to the *ac* plane and a 3D network of vanadium(IV) selenite with two types of tunnels along the *a* axis (a) and a 1D chain of zinc(II) selenite along the *a* axis (b) in ZnVSe$_2$O$_7$.

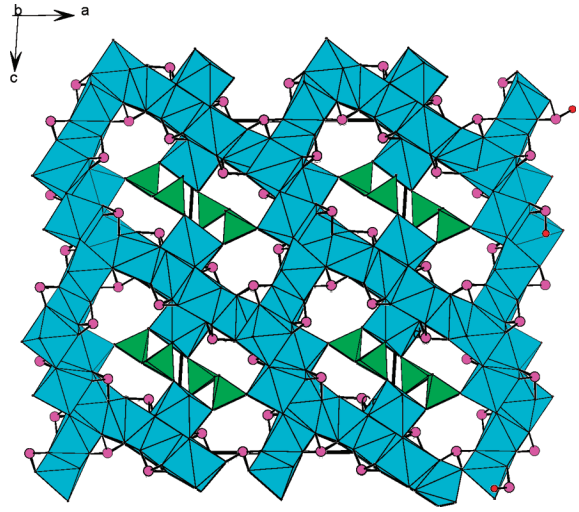

Figure 3. View of the structure of Cd$_6$V$_2$Se$_5$O$_{21}$ down the *b* axis. The VO$_4$ tetrahedra are shaded in green, and CdO$_6$, CdO$_7$, and CdO$_5$ polyhedra in cyan. Selenium and oxygen atoms are drawn as pink and red circles, respectively.

groups and two O^{2-} anions. The V−O bond distances are in the range of 1.610(3)−2.318(3) Å. Hence, the VO$_6$ octahedron is severely distorted. The vanadium(IV) cation is distorted toward a corner (O(7), local C_4 direction) with one short (1.610(3) Å), four normal (1.965(3)−2.007(2) Å), and one long (2.318(3) Å) V−O bonds (Table 2), such a type of distortion for a vanadium(IV) cation has been also reported in VO(SeO$_3$)·H$_2$O, Cu(VO)(SeO$_3$)$_2$, and the V^{4+}/V^{5+} mixed-valent KV$_2$SeO$_7$, in which the pentavalent vanadium is tetrahedrally coordinated.[15,16] Both selenium(IV) cations are coordinated by three oxygen atoms in a distorted Ψ-SeO$_3$ tetrahedral geometry with the forth site occupied by the lone-pair electrons. The Se−O distances fall in the range of 1.655(2) to 1.746(2) Å. The two selenite groups adopt two different coordination modes. The Se(1)O$_3$ group chelates with a zinc(II) ion bidentately and also bridges with another zinc(II) ion and two vanadium(IV) cations, whereas the Se(2)O$_3$ group forms two Se−O−Zn and two Se−O−V bridges. Results of bond-valence calculations indicate that both the vanadium and selenium atoms are in an oxidation state of +4. The calculated total bond valences are 4.15, 4.00, and 4.07, respectively for V(1), Se(1), and Se(2).[17] The assignment of the oxidation of +4 for the vanadium is also supported by its room-temperature EPR spectrum, which shows a typical *g* value of 1.9580.

The VO$_6$ octahedra are interconnected via corner-sharing (O(7)) into a 1D chain along the <101> directions (part a of Figure 2). The V−O(7)−V bond angle is 164.8(2)° with a V···V separation of 3.8943(4) Å. These vanadium oxide chains are further bridged by Se(1)O$_3$ groups into a 2D layer parallel to the *ac* plane (part a of Figure 2). Such 2D layers are further interconnected by bridging Se(2)O$_3$ groups into a pillar-layered architecture with two types of tunnels of six member rings along the *a* axis (part a of Figure 2). Both 6MR are composed of four VO$_6$ octahedra and two SeO$_3$ groups, one is more wider whereas the other one is more narrow, with the lone pairs of the selenium(IV) pointing toward its center (part a of Figure 2). The zinc(II) cations are located at the wider tunnels (part a of Figure 1).

Two [Zn(1)O$_5$] polyhedra are interconnected via edge-sharing (O(6)···O(6)) into a dimeric unit with a Zn(1)−O(6)−Zn(1) bond angle of 101.0(1)°. Each pair of such dimeric units are linked by a pair of bridging and chelating Se(1)O$_3$ groups into a 1D chain along the *a* axis. The Se(2)O$_3$ groups are grafted onto the chain via corner-sharing, resulting in a $[ZnSe_2O_6]^{2-}$ anionic chain (part b of Figure 2). The Zn−O−Se bond angles range from 99.9(1) to 131.1(2)°.

It should be noted that the structure of ZnVSe$_2$O$_7$ is different from those of two forms of CuVSe$_2$O$_7$ reported

(16) (a) Millet, P.; Enjalbert, R.; Galy, J. *J. Solid State Chem.* **1999**, *147*, 296. (b) Lee, K.-S.; Kwon, Y.-U.; Namgung, H.; Kim, S.-H. *Inorg. Chem.* **1995**, *34*, 4178.

(17) (a) Brown, I. D.; Altermatt, D. *Acta Crystallogr.* **1985**, *B 41*, 244. (b) Brese, N. E.; O'Keeffe, M. *Acta Crystallogr.* **1991**, *B 47*, 192.

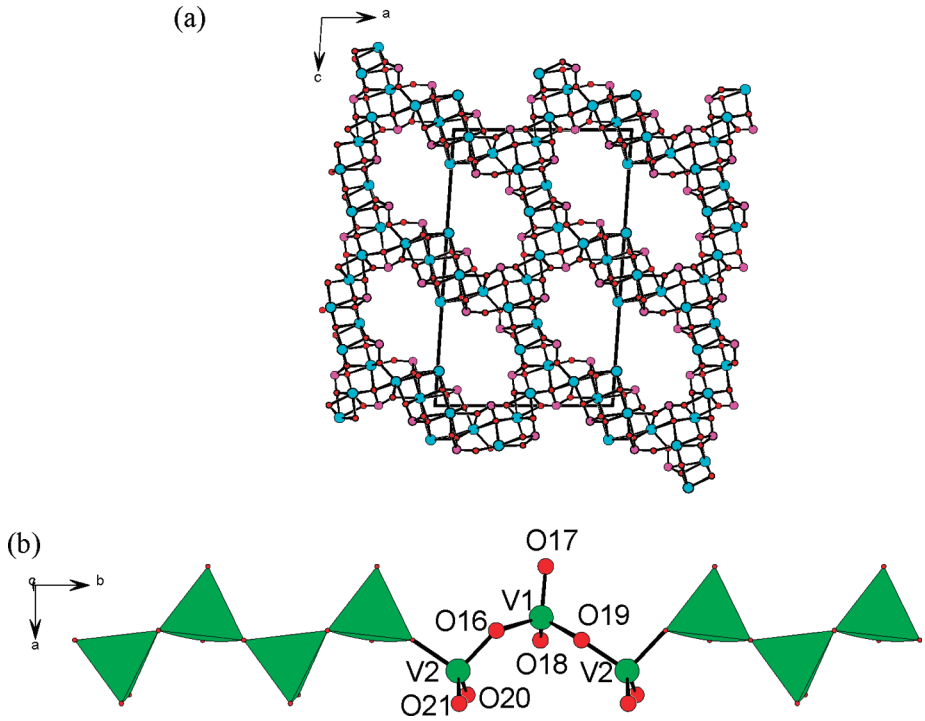

Figure 4. A 3D cationic framework of cadmium selenite showing large tunnels along the *b* axis (a) and a 1D vanadium oxide chain along the *b* axis (b) in $Cd_6V_2Se_5O_{21}$.

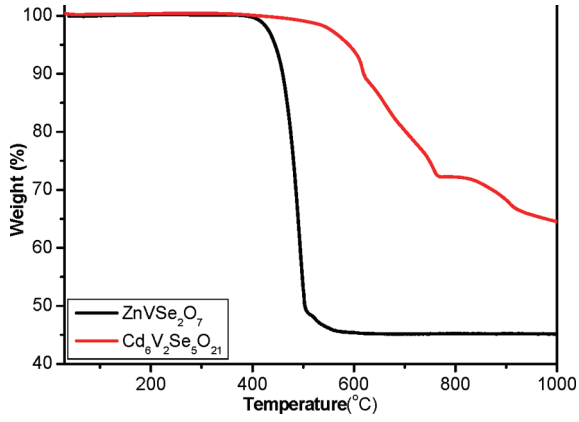

Figure 5. TGA curves for $ZnVSe_2O_7$ and $Cd_6V_2Se_5O_{21}$.

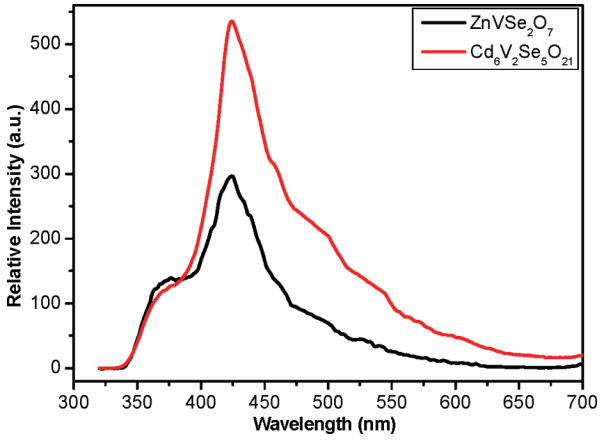

Figure 6. Emission spectra of $ZnVSe_2O_7$ and $Cd_6V_2Se_5O_{21}$ under λ_{ex} = 290 nm.

(monoclinic and orthorhombic phases),[16a] although their structural formulas are quite similar. In both forms of

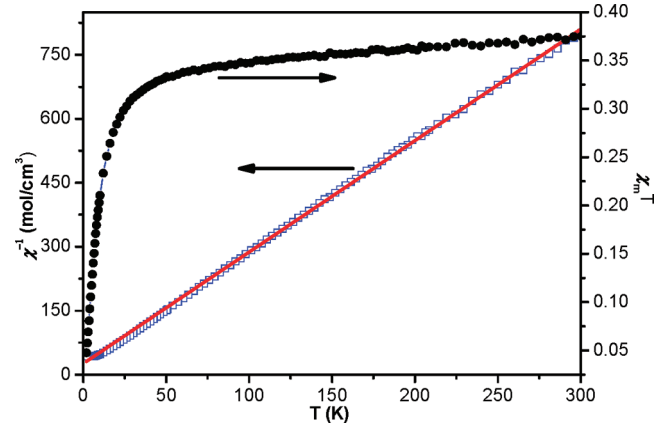

Figure 7. χ^{-1} versus T and χT versus T plots for $ZnVSe_2O_7$. The red line represents the linear fit of data according to the Curie−Weiss Law.

$CuVSe_2O_7$, both CuO_6 and VO_6 octahedra are severely distorted. In the monoclinic form, each pair of CuO_6 and VO_6 octahedra is interconnected into $[Cu_2O_{10}]$ and $[V_2O_{10}]$ dimers via sharing edges. These dimers are further bridged by interconnected via corner-sharing (V−O−Cu bridges) into a layered structure with the selenite groups capping on both sides of the layer. The lone pairs of the Se(IV) cations are orientated toward the interlayer space. In the orthorhombic phase, the CuO_6 and VO_6 octahedra are also interconnected via edge- and corner-sharing into a 2D copper vanadium oxide layer with 6 MRs in the *ab* plane. These 2D layers are bridged by the SeO_3 groups into a 3D layer-pillared structure.[16a]

The structure of $Cd_6V_2Se_5O_{21}$ features a novel 3D network built by 3D frameworks of cadmium(II) selenite and the 1D chains of corner-sharing V^VO_4 tetrahedra that are interconnected via Cd−O−V bridges (Figure 3). The synthesis of

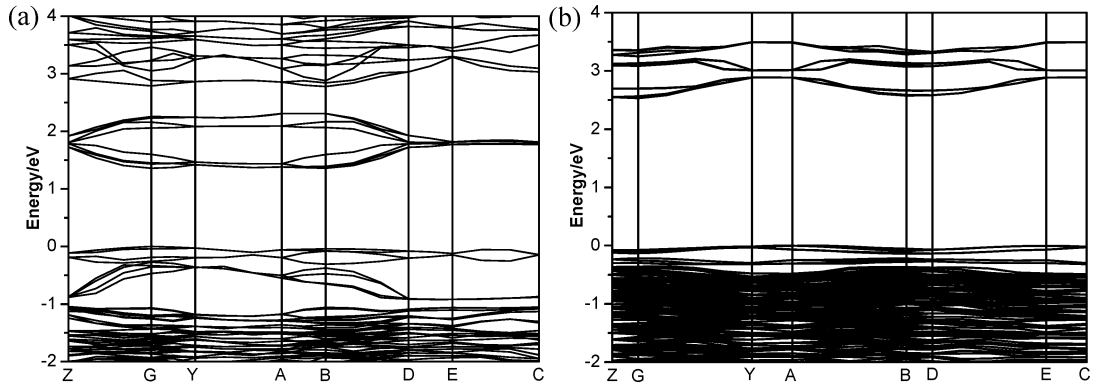

Figure 8. Band structures of $ZnVSe_2O_7$ and $Cd_6V_2Se_5O_{21}$ in the range of −2.0 and 4.0 eV. The Fermi level is set at 0 eV.

Table 3. State Energies (eV) of the Lowest Conduction Band (L-CB) and the Highest Valence Band (H-VB) at Some k-Points of the Crystals $ZnVSe_2O_7$ and $Cd_6V_2Se_5O_{21}$

	$ZnVSe_2O_7$		$Cd_6V_2Se_5O_{21}$	
k-point	L-CB	H-VB	L-CB	H-VB
Z (0.000, 0.000, 0.500)	1.72341	−0.11095	2.54852	−0.07209
G (0.000, 0.000, 0.000)	1.36074	0	2.53299	−0.07228
Y (0.000, 0.500, 0.000)	1.41783	−0.02753	2.88512	−0.01528
A (−0.500, 0.500, 0.000)	1.37988	−0.06091	2.88245	−0.00143
B (−0.500, 0.000, 0.000)	1.35798	−0.04263	2.57564	−0.05107
D (−0.500, 0.000, 0.500)	1.72167	−0.08020	2.58170	−0.06840
E (−0.500, 0.5000, 0.500)	1.76967	−0.12176	2.88271	−0.00181
C (0.000, 0.500, 0.500)	1.76961	−0.14258	2.88586	−0.01909

$Cd_6V_2Se_5O_{21}$ can be expressed by the following reaction at 650 °C: $6CdO + V_2O_5 + 5SeO_2 \rightarrow Cd_6V_2Se_5O_{21}$. $Cd_6V_2Se_5O_{21}$ can be also formulated as $Cd_6(V_2O_6)(SeO_3)_5$. Among six unique cadmium(II) ions in an asymmetric unit, four of them are octahedrally coordinated by six oxygen atoms: Cd(1) surrounded by three oxygens from three selenite groups and three O^{2-} anions; Cd(2) coordinated by six oxygen atoms from five selenite groups (one bidentate chelation and four unidentate) with one Cd−O bond elongated (Cd(2)−O(12) 2.671(6) Å); Cd(5) and Cd(6) each is coordinated by six oxygens from six selenite groups. Cd(3) is seven-coordinated by six oxygens from five selenite groups (one bidentate chelating and four unidentate) and one O^{2-} anion, whereas Cd(4) is eight-coordinated by eight oxygens from five selenite groups (three in bidentate chelating fashion and two in unidentate fashion). The Cd−O distances are in the range of 2.191(7) to 2.671(6) Å (Table 2), which are comparable to those reported in other cadmium(II) selenites or tellurites.[10b] Both vanadium(V) cations are in a slightly distorted tetrahedral coordination environment with V−O distances in the range of 1.638(6) to 1.795(6) Å (Table 2), which are comparable to those reported in other vanadium selenites or tellurites.[7,10] All five selenium(IV) atoms adopt the same asymmetric coordination geometry, and each is coordinated by three oxygen atoms in a distorted Ψ-SeO_3 tetrahedral geometry with the forth site occupied by the lone-pair electrons. The Se−O bond distances are in the range of 1.682(6) to 1.739(6) Å, which are close to those in $ZnVSe_2O_7$. Results of bond-valence calculations indicate that the vanadium atoms are in an oxidation of +5 and the selenium atoms are +4. The calculated total-bond valences

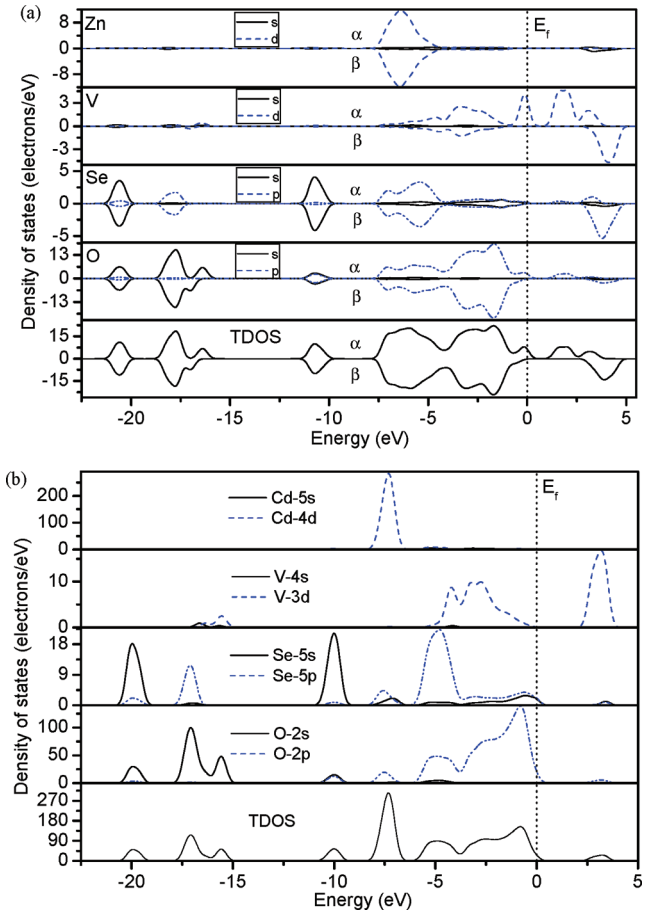

Figure 9. Total and partial DOS of $ZnVSe_2O_7$ (a) and $Cd_6V_2Se_5O_{21}$ (b). α and β represent spin up and spin down, respectively. The Fermi level is set at 0 eV.

are 5.19, 5.13, 4.01, 3.98, 4.01, 4.04, and 4.03, respectively, for V(1), V(2), Se(1), Se(2), Se(3), Se(4), and Se(5).[17]

The five selenite groups are solely bond to the cadmium(II) ions and adopt four different coordination modes. The $Se(1)O_3$ and $Se(4)O_3$ groups adopt a same coordination fashion, each forms a bidentate chelation with a cadmium(II) ion and also bridges to five other cadmium(II) ions, two oxygen atoms are bidentate, whereas the third one is tridentate. The $Se(2)O_3$ group chelates bidentately with a cadmium(II) and also bonds with four other cadmium(II) ions, one oxygen atom is unidentate, one is bidentate,

whereas the third one is tridentate. The $Se(3)O_3$ group forms two chelating rings with two cadmium(II) ions and also bridges to four other cadmium(II) ions, and all three oxygens are tridentate. The $Se(5)O_3$ group is heptadentate and bridges with seven cadmium(II) ions, two oxygen atoms are bidentate, whereas the third one is tridentate.

The cadmium(II) ions are interconnected by bridging and chelating selenite groups into a 3D framework with large tunnels along the *b* axis, the size of tunnel is estimated to be 3.0 × 12.0 $Å^2$ based on the structural data (the atomic radii of the ring atoms have been deducted, part a of Figure 4). The tunnels are constructed by 16-MRs composed of 6 SeO_3 groups and 10 cadmium atoms. The lone-pair electrons of the selenite groups are pointing toward the centers of the above tunnels. The effective volume of the lone pair is approximately the same as the volume of an O^{2-} anion according to Galy and Andersson.[18] Neighboring VO_4 tetrahedra are interconnected via corner-sharing into a 1D $\{V_2O_6\}^{2-}$ anionic chain along the *b* axis (part b of Figure 4). These vanadium oxide chains are inserted in the above tunnels of the cadmium(II) selenite and interact with the main skeleton via V−O−Cd bridges (Figure 3).

It should be mentioned that the structure of $Cd_6V_2Se_5O_{21}$ is somehow similar to that of $Nd_4Cu(TeO_3)_5Cl_3$.[19] The latter contains large 16 MR tunnels of neodymium(III) tellurite, which are inserted by 1D chains of corner-sharing $CuCl_4$ tetrahedra.[19]

Thermogravimetric Analyses. TGA analyses under an air atmosphere indicate that $ZnVSe_2O_7$ and $Cd_6V_2Se_5O_{21}$ are stable up to 390 and 350 °C, respectively (Figure 5). $ZnVSe_2O_7$ exhibits only one main step of weight loss in the temperature range of 390−650 °C, which corresponds to the release of 2 molar of SeO_2 per formula unit and the slight weight gain of the oxidation of vanadium(IV) to vanadium(V) under air. Above 650 °C, the weight remains almost unchanged. Powder X-ray diffraction studies indicate that the final residual is $Zn_2V_2O_7$ (Supporting Information).[20] The observed weight loss of 54.8% is close to the calculated one (55.4%). For $Cd_6V_2Se_5O_{21}$, the decomposition continues up to 1000 °C, the weight loss corresponds to liberation of SeO_2 molecules. The total weight loss at 1000 °C is 35.8%, and the decomposition is incomplete based on the slope of its TGA curves. The final residual for $Cd_6V_2Se_5O_{21}$ was not characterized due to the incompleteness of its decomposing.

Optical Properties. IR studies indicate that both compounds have little absorptions in the range of 4000 to 1000 cm^{-1}. The IR absorption bands at 999, 927, and 876 cm^{-1} for $ZnVSe_2O_7$, and 953, 935, 917, 905, 848, and 820 cm^{-1} for $Cd_6V_2Se_5O_{21}$ are due to υ(V=O) or υ(V−O−V) vibrations, whereas those at 751, 675, 614, 532, 487, 452, and 414 cm^{-1} for $ZnVSe_2O_7$, and 787, 724, 699, 638, 488 and 470 cm^{-1} for $Cd_6V_2Se_5O_{21}$ can be assigned to the vibrations of υ(V−O), υ(Se−O), υ(Se−O−Se) and υ(Se−O−V).[10b,21] Both the emission spectra of $ZnVSe_2O_7$ and $Cd_6V_2Se_5O_{21}$ show a broad emission band at around 424 nm under the excitation at 290 nm (Figure 6), respectively, which may be attributed to the LMCT.[10b,22]

Magnetic Properties. Because $ZnVSe_2O_7$ contains one paramagnetic V^{4+} ion (d^1), its magnetic property was studied. $ZnVSe_2O_7$ obeys the Curie−Weiss Law in the temperature range of 50−300 K, and below 50 K a slight deviation was observed (Figure 7). At 300 K, the $\chi_M T$ value of 0.38 emu·mol^{-1}·K corresponds to an effective magnetic moment (μ_{eff}) of 1.74 μ_B for an noninteracting V^{4+} ($3d^1$, $S = {}^1/_2$, $g =$ 1.9580 for V^{4+} from EPR result) ion per formula unit.[15,16] The $\chi_M T$ value decreased slightly upon cooling in the range of 50 to 300 K. Below 50 K, it decreases more rapidly upon cooling and reaches a value of 0.047 emu·mol^{-1}·K at 2.0 K. A linear fit of the magnetic data in the range of 50−300 K gave a Weiss constant (θ) of −9.93(2) K, indicating significant antiferromagnetic interactions between magnetic centers. The magnetic interaction is expected to be dominated by magnetic exchange interaction between two vanadium(IV) ions connected via V−O−V bridges (V···V 3.897(1) Å, V−O−V 165.09(2)°) within the vanadium oxide chain. The interchain magnetic interactions between vanadium(IV) centers interconnected via a V−O−Se−O−V bridges are expected to very weak due to much larger V···V separations (at least 6.284(1) Å).

Theoretical Studies. To further understand the chemical bonding and electronic structures of both compounds, band structures as well as density of states (DOS) calculations based on the DFT method were made by using the computer code *CASTEP*.[13]

The calculated band structures of $ZnVSe_2O_7$ and $Cd_6V_2Se_5O_{21}$ along high-symmetry points within the first Brillouin zone are plotted in Figure 8. It is found that the top of valence bands (VBs) is almost flat, whereas the bottom of conduction bands (CBs) displays some dispersion for both compounds. The state energies (eV) of the lowest conduction band (L-CB) and the highest valence band (H-VB) at some k points of both compounds are listed in Table 3. For $ZnVSe_2O_7$, the lowest energy of the CBs at the B point is 1.358 eV, whereas the highest energy (0.0 eV) of VBs is located at the G point. Therefore, $ZnVSe_2O_7$ displays an indirect band gap of 1.36 eV. For $Cd_6V_2Se_5O_{21}$, the lowest energy at the CBs (2.53 eV) of VBs is located at the G point, whereas the highest energy of VBs at both the A and E points is a very close value of 0.0 eV; hence, $Cd_6V_2Se_5O_{21}$ has an indirect band gap of 2.53 eV, which is much larger than that of $ZnVSe_2O_7$. The absorption edges of $ZnVSe_2O_7$ and $Cd_6V_2Se_5O_{21}$ are about 1555 (0.80 eV) and 580 nm (2.14 eV), respectively. Hence, our calculated band gaps are

(18) Galy, J.; Meunier, G.; Andersson, S.; Åström, A. *J. Solid State Chem.* **1975**, *13*, 142.
(19) Shen, Y.-L.; Mao, J.-G. *Inorg. Chem.* **2005**, *44*, 5328.
(20) Gopal, R.; Calvo, C. *Can. J. Chem.* **1973**, *51*, 1004.
(21) (a) Sivakumar, T.; Ok, K. M.; Halasyamani, P. S. *Inorg. Chem.* **2006**, *45*, 3602. (b) Lu, Y.; Wang, E. B.; Yuan, M.; Luan, G. Y.; Li, Y. G.; Zhang, H.; Hu, C. W.; Yao, Y. G.; Qin, Y. Y.; Chen, Y. B. *Dalton Trans.* **2002**, 3029. (c) Xiao, D. R.; Wang, S. T.; Wang, E. B.; Hou, Y.; Li, Y. G.; Hu, C. W.; Xu, L. *J. Solid State Chem.* **2003**, *176*, 159.
(22) (a) Liu, C. S.; Shi, X. S.; Li, J. R.; Wang, J. J.; Bu, X. H. *Cryst. Growth Des.* **2006**, *6*, 656. (b) Guo, Z. G.; Cao, R.; Li, X. J.; Yuan, D. Q.; Bi, W. H.; Zhu, X. D.; Li, Y. F. *Eur. J. Inorg. Chem.* **2007**, 742.

slightly larger than the experimental results. The overestimation of band gaps by the DFT calculations has been also reported in other inorganic compounds.[23]

The bands can be assigned according to the total and partial densities of states (DOS) as plotted in Figure 9. The TDOS and PDOS of both compounds are quite similar. The bands just above the Fermi level are derived from V-3d, Se-4p, and O-2p states in 0.9−5.0 eV and 2.0−4.1 eV, respectively, for $ZnVSe_2O_7$ and $Cd_6V_2Se_5O_{21}$. The VBs just below the Fermi level are mainly from O-2p and V-3d states mixing with a small amount of the Se-4s and Se-4p states in both compounds. The states of O-2s and Se-4s dominate the VB, ranging from −21.4 to −9.1 eV, whereas the VBs ranging from −7.9 eV (−8.5 eV for $Cd_6V_2Se_5O_{21}$) to the Fermi energy are mainly composed of the states of O-2p, Zn-3d (or Cd-4d), Se-4p, and V-3d states. Inspecting the spin splitting near the Fermi level, a small splitting is observed in $ZnVSe_2O_7$, which is in good agreement with the effective magnetic moment (1.74 μ_B) from magnetic measurements.

In addition, we calculated the atomic site and angular momentum projected DOS of the two compounds to elucidate the nature of the electronic band structures and chemical bonds. As shown in Figure 9, it can be observed that the densities of Zn-3d (or Cd-4d) states are larger than those of the O-2p states from −7.8 to −4.3 eV (−8.5 to −6.2 eV for $Cd_6V_2Se_5O_{21}$), whereas the densities of V-3d and Se-4p states are much smaller than those of O-2p states from −8.0 to −0.8 eV, which indicate that the covalent interactions in Zn−O and Cd−O bonds is not as strong as that in V−O and Se−O bonds. In other words, the V−O and Se−O bonds are mainly covalent in character, whereas the Zn−O and Cd−O bonds are mainly ionic in character.

Semiempirical population analyses allow for a more quantitative bond analysis. The calculated bond orders of Zn−O, V−O, and Se−O bonds are 0.17−0.31 e, 0.16−0.90 e, and 0.30−0.46 e (covalent single-bond order is generally 1.0 e), respectively for $ZnVSe_2O_7$. It is obviously observed that the overlap populations have the following order: elongated V−O bond < normal V−O bonds < short V−O bond (Supporting Information). The calculated bond orders for Cd−O, V−O and Se−O bonds are 0.07−0.27 e, 0.57−0.93 e, and 0.40−0.56 e, respectively, for $Cd_6V_2Se_5O_{21}$ (Supporting Information). Accordingly, we can also say that the covalent character of the V−O bond is larger than that of the Se−O bond, and the ionic character of the Zn−O or Cd−O bond is larger than that of the Se−O bond.

(23) (a) Zhu, J.; Cheng, W.-D.; Wu, D.-S.; Zhang, H.; Gong, Y.-J.; Tong, H.-N. *J. Solid State Chem.* **2006**, *179*, 597. (b) Zhu, J.; Cheng, W.-D.; Wu, D.-S.; Zhang, H.; Gong, Y.-J.; Tong, H.-N.; Zhao, D. *Eur. J. Inorg. Chem.* **2007**, 285.

Conclusions

In summary, the syntheses, band and crystal structures, and properties of two new zinc(II) and cadmium(II) vanadium selenites have been described. The structure of $ZnVSe_2O_7$ can be viewed as the zinc(II) cations being located at the 1D tunnels of the 3D vanadium(IV) selenite, whereas the structure of $Cd_6V_2Se_5O_{21}$ can be considered as a 3D framework of cadmium(II) selenite with large tunnels filled by 1D chains of corner-sharing V^VO_4 tetrahedra. Under hydrothermal conditions, vanadium(V) is prone to be reduced to vanadium(IV). The vanadium(IV) centers in $ZnVSe_2O_7$ interact antiferromagnetically. It is expected that a variety of new compounds with new types of structures and interesting physical properties can be discovered in the transition-metal−vanadium selenite or tellurite systems by hydrothermal or solid-state synthetic technique.

Acknowledgment. This work was supported by National Natural Science Foundation of China (grants 20731006, 20573113, and 20521101), the Knowledge Innovation Program of the Chinese Academy of Sciences, and Key project of the Chinese Academy of Sciences (grant KJCX2-YW-H01).

Supporting Information Available: X-ray crystallographic files in CIF format, calculated bond orders, UV spectra, and simulated and experimental XRD powder patterns for $ZnVSe_2O_7$ (as well as its decomposition residual) and $Cd_6V_2Se_5O_{21}$. This material is available free of charge via the Internet at http://pubs.acs.org.

IC800638E